

# 全球モデルによる エアロゾル間接効果の評価の現状と展望

竹村 俊彦（九州大学応用力学研究所）

## *Outline*

大気大循環モデルを用いた雲エアロゾル相互作用の研究の現状と問題点を紹介することにより、様々なツールを用いて様々な方向から雲へアプローチしている研究を今後どのように融合させていくかを議論するための材料を提供する。

# Introducti

on

気候変動は地球規模の問題であるため、統合的な研究においては全球モデルが主要ツールとなっている。しかし、雲過程は地球放射収支を左右する重要部分であるにもかかわらず、全球モデルでは十分な表現をしているとは言えない。

- ・ 全球モデルでは雲エアロゾル微物理過程を表現するための時空間分解能が不足
- ・ 雲過程を統合的に表現するには依然として計算機リソースが不足
- ・ 雲エアロゾル微物理過程自体に未解明の部分が存在（特に氷晶過程）

→ 研究者個々人の興味ある方向（力学・放射・微物理）から様々なスケールで雲過程にアプローチしてきた。

しかし、自然現象として各プロセスは切り分けられるものではない。

→ 様々なアプローチの方法があるが、相互に意識はしてきたはずである。

将来的には、これまでに研究されてきた各プロセスの理解の蓄積をベースとして、各プロセスが融合していくことが自然な流れであり理想である。

気候モデルの観点からは、

- ・ 水－雲－気候フィードバック過程に対する理解の向上
- ・ モデルの精度向上・不確定性の明確化

が期待される。



## **Global three-dimensional simulation of aerosol optical thickness distribution of various origins**

Toshihiko Takemura,<sup>1</sup> Hajime Okamoto,<sup>2</sup> Yoshihiro Maruyama,<sup>1</sup> Atusi Numaguti,<sup>3</sup> Akiko Higurashi,<sup>4</sup> and Teruyuki Nakajima<sup>1</sup>

**Abstract.** A global three-dimensional model that can treat transportation of various species of aerosols in the atmosphere is developed using a framework of an atmospheric general circulation model (AGCM). Main aerosols in the troposphere, i.e., soil dust, carbonaceous (organic and black carbon), sulfate, and sea-salt aerosols, are introduced into this model. Prior to the model calculations the meteorological parameters are calculated by the AGCM with the nudging technique using reanalysis data. To evaluate aerosol effects on the climate system and to compare simulated results with observations, the optical thickness and Ångström exponent are also calculated taking into account the size distribution and composition. The model results are validated by both measured surface aerosol concentrations and retrieved aerosol optical parameters from National Oceanic and Atmospheric Administration/Advanced Very High Resolution Radiometer. A general agreement is found between the simulated result and the observation globally and seasonally. One of the significant results is that the simulated relative contribution of anthropogenic carbonaceous aerosols to the total optical thickness is comparable to that of sulfate aerosols at midlatitudes of the Northern Hemisphere, which agrees with recent observations. This result leads to a conclusion that the radiative effect evaluation of aerosols on the climate system is necessary to be modified because optical properties of carbonaceous aerosols are different from those of sulfate aerosols. The other finding is that the seasonal shift off the west coast of North Africa observed by satellites, i.e., the latitude of the maximum optical thickness moves seasonally, is also reproduced in consideration of a mixed state of soil dust and carbonaceous aerosols.

**Meteorological field**  
(wind, temperature, etc.)

on/off

**General circulation model**

**Aerosol transport processes**  
emission, advection, diffusion, chemical  
reaction, deposition (wet, dry)

**Aerosol optical properties**  
**Aerosol direct and indirect effects**

**Aerosol global distribution**  
**Evaluation of aerosol effects on  
climate system**

§ Coupled to CCSR/NIES/FRCGC AGCM

§ Tracers: black carbon (BC), organic carbon (OC), sulfate, soil dust, sea salt, SO<sub>2</sub>, DMS

§ Emission

- BC, OC: biomass burning, fossil fuel, biofuel, agricultural activity, terpene
- SO<sub>2</sub>: fossil fuel, biomass burning, volcano
- DMS: phytoplankton, land vegetation, soil
- Soil dust: online calculation with wind speed near surface, vegetation, soil moisture, snow amount
- Sea salt: online calculation with wind speed near surface

§ Advection

Flux-Form Semi-Lagrangian (FFSL) method  
Arakawa-Schubert cumulus convection

§ Diffusion

§ Chemical reaction (sulfur)

- Gas phase:  $\text{DMS} + \text{OH} \rightarrow \text{SO}_2$ ,  $\text{SO}_2 + \text{OH} \rightarrow \text{SO}_4^{2-}$
- Liquid phase:  $\text{S(IV)} + \text{O}_3 \rightarrow \text{SO}_4^{2-}$ ,  $\text{S(IV)} + \text{H}_2\text{O}_2 \rightarrow \text{SO}_4^{2-}$
- OH, O<sub>3</sub>, H<sub>2</sub>O<sub>2</sub>: CHASER (Sudo et al. 2002)
- Deposition
- Wet deposition
- Re-emission by evaporation of rain
- Dry deposition
- Gravitational settling

Takemura et al. (JGR, 105, 17853-17873, 2000)

Takemura et al. (J. Climate, 15, 333-352, 2002)

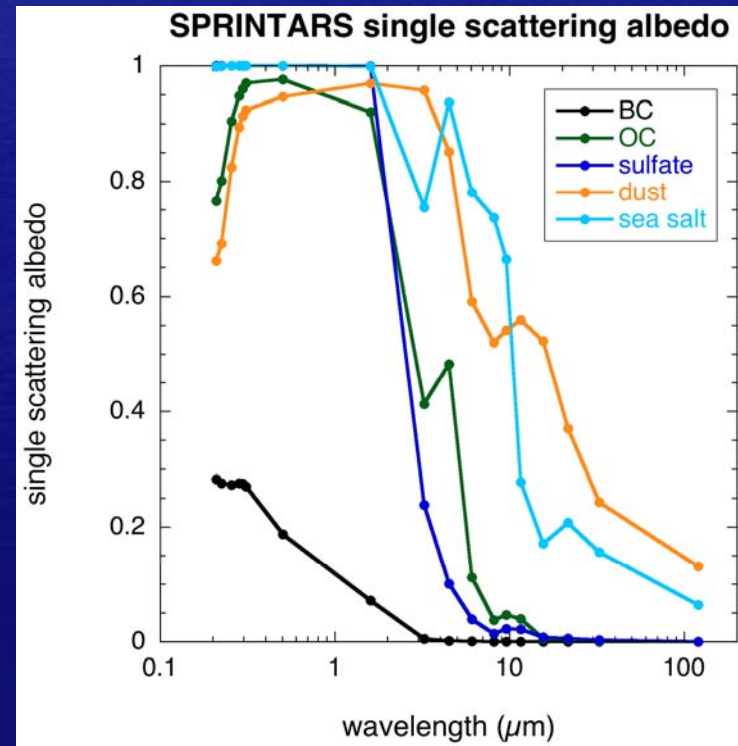
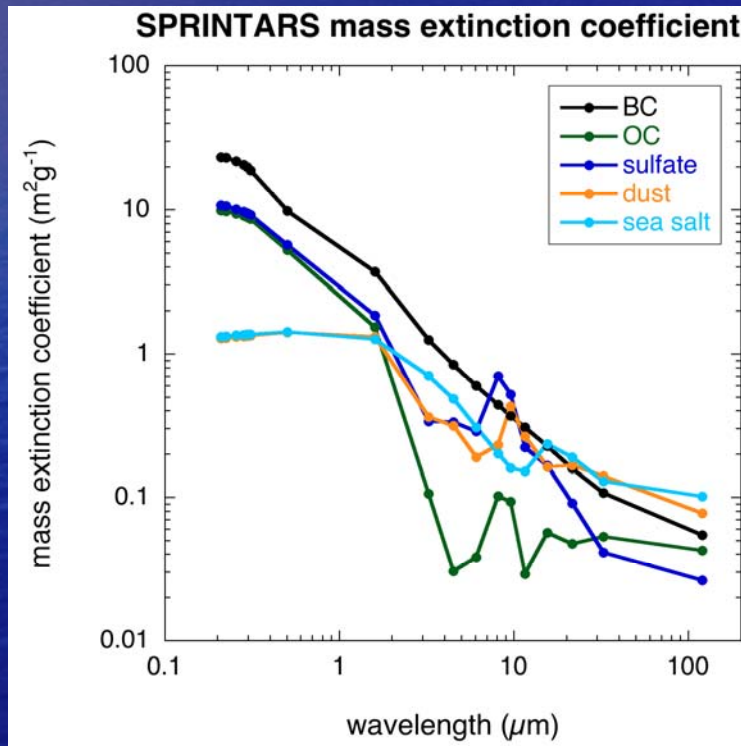
Takemura et al. (JGR, 110, 2004JD005029, 2005)



# Model

## description Aerosol direct effect

- Aerosol transport processes are coupled to the radiation process in *GCM* considering refractive indices, size distributions, and hygroscopic growth of each aerosol component.
- Semi-direct effect is included if meteorological field is calculated online.



Wavelength dependences of mass extinction coefficient (left) and single scattering albedo (right) for water and dry particles of each aerosol species.

# Model

## description

### Aerosol indirect

#### effect

#### § Cloud droplet number concentration

$$N_c = N_a \left[ 1 + \left\{ f_1(\sigma_a) \left( \frac{AN_a\beta}{3\alpha\omega} \right)^2 + f_2(\sigma_a) \frac{2A^3 N_a \beta \sqrt{G}}{27 Br_m^3 (\alpha\omega)^{3/2}} \right\}^{b(\sigma_a)} \right]^{-1}$$

*Abdul-Razzak et al. (2000), Ghan et al. (1997)*

$N_a$ : Aerosol particle number concentration

$r_m$ : Mode radius of aerosol size distribution

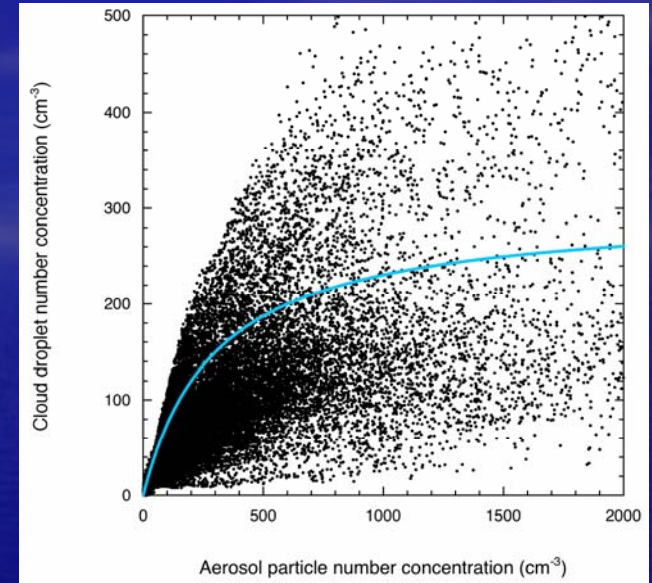
$\sigma_a$ : Standard deviation of aerosol size distribution

$A$ : Curvature effect

$B$ : Solute effect

$\omega$ : Updraft velocity

$$\bar{\omega} + c\sqrt{TKE}$$



Relationship between the number concentrations of aerosol particles ( $r > 0.05 \mu\text{m}$ ) and cloud droplets. Blue line shows the relationship in past GCM studies.

#### § Cloud droplet effective radius $r_{eff}$ → 1st indirect effect

$$r_{eff} = k \left( \frac{3}{4\pi\rho_w} \frac{\rho l}{N_c} \right)^{\frac{1}{3}}$$

$\rho l$ : Cloud water content  
 $\rho_w$ : Water density

#### § Precipitation rate $P$

$$P = -\frac{dl}{dt} = \frac{\alpha \rho l^2}{\beta + \gamma \frac{N_c}{\rho l}}$$

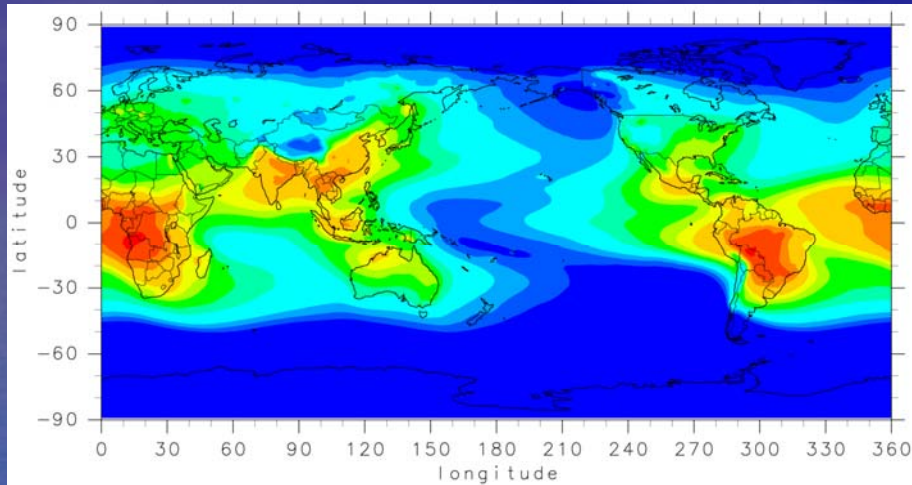
#### → 2nd indirect effect

$\alpha, \beta, \gamma$ : Constants



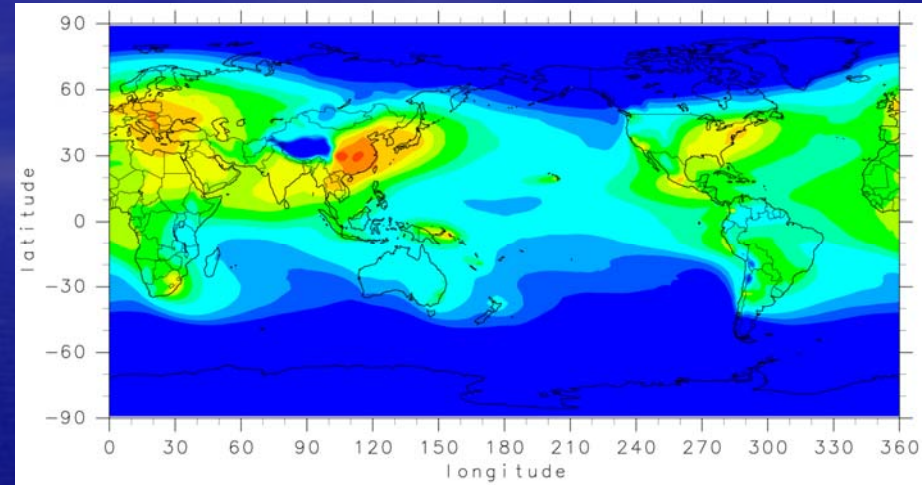
# Global aerosol distributions

BC + OC

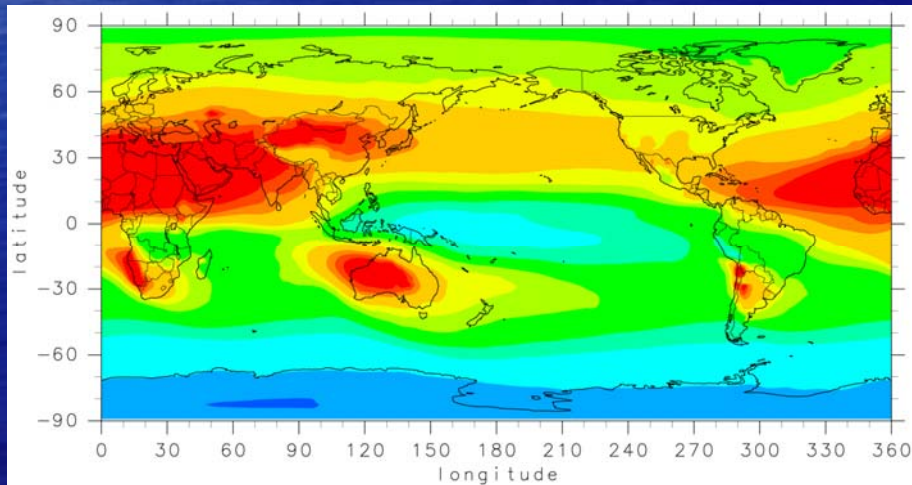


Column loading

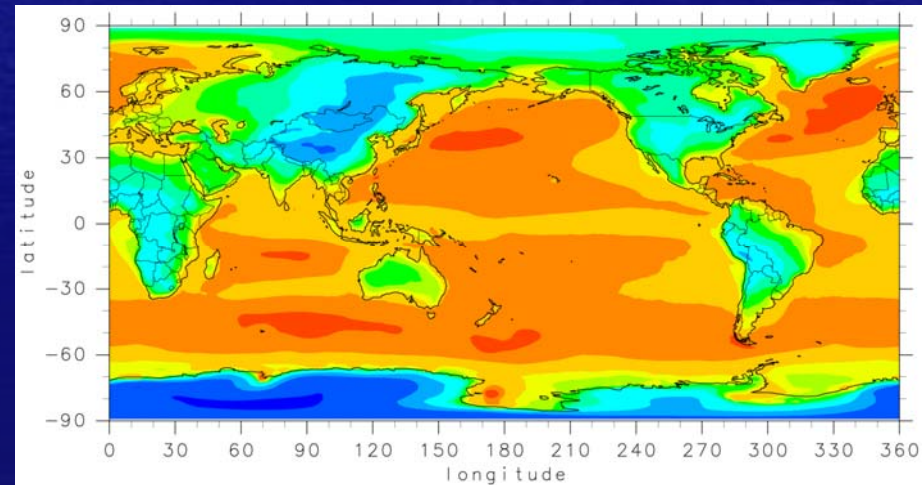
Sulfate



Soil dust



Sea salt

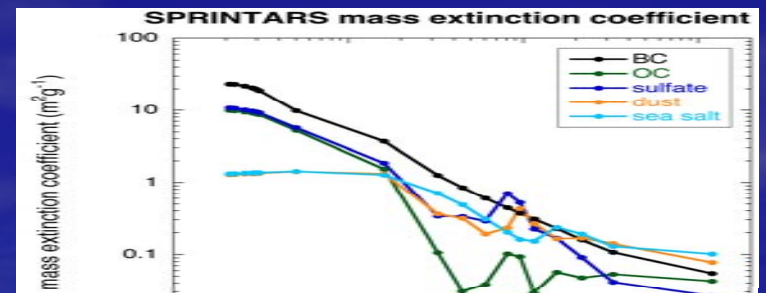
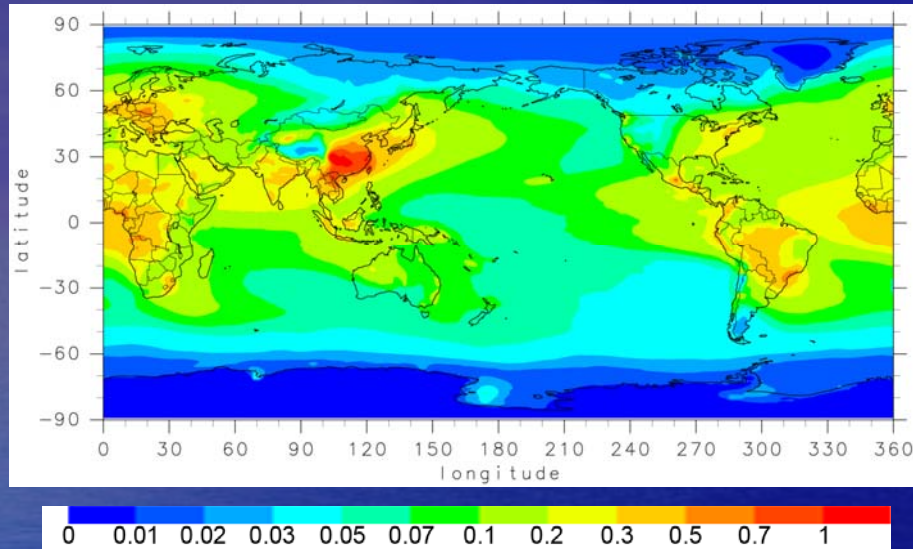


0 0.5 0.7 1 2 3 5 7 10 20 30 50 ( $\text{mg m}^{-2}$ )

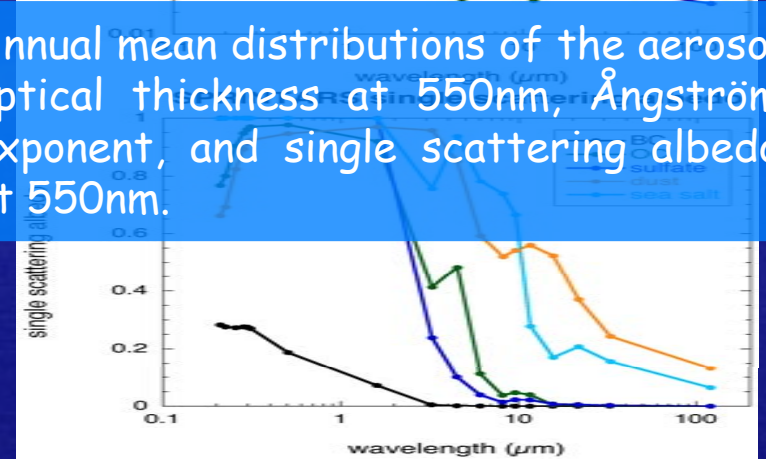
Annual mean distributions of the mass column loading for each aerosol component.

# Aerosol optical properties

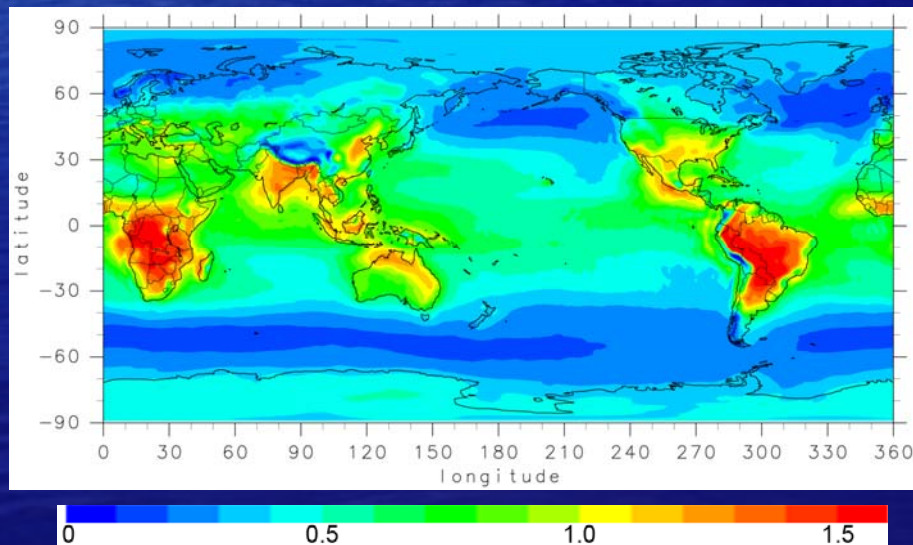
Optical thickness (550nm)



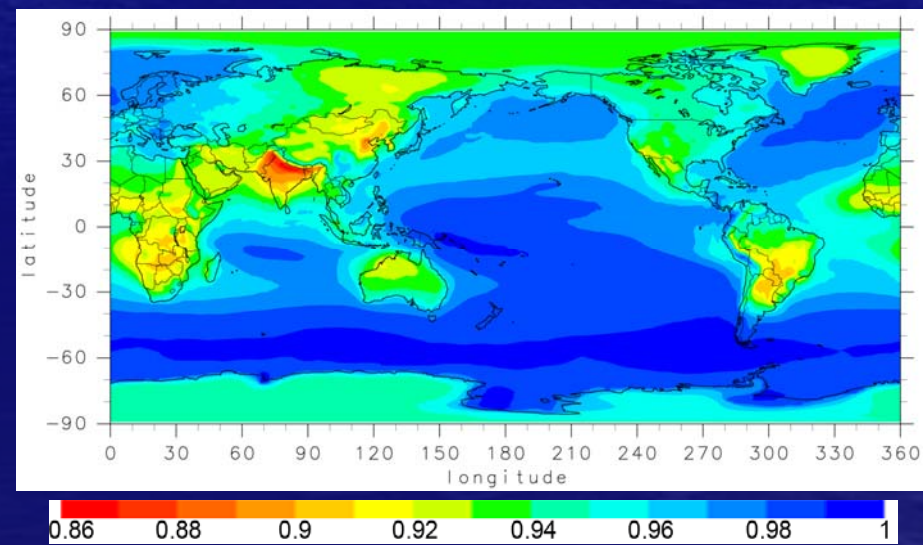
Annual mean distributions of the aerosol optical thickness at 550nm, Ångström exponent, and single scattering albedo at 550nm.



Ångström exponent (550 – 860nm)



Single scattering albedo (550nm)





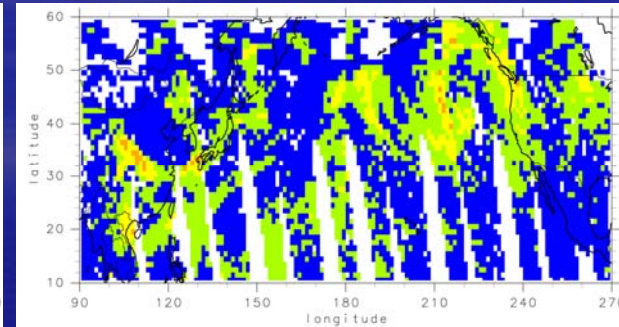
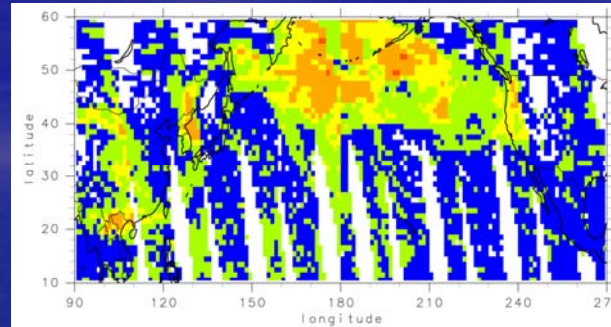
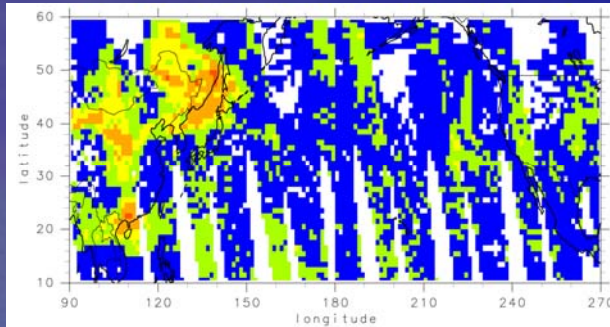
# Asian dust

storm April 8

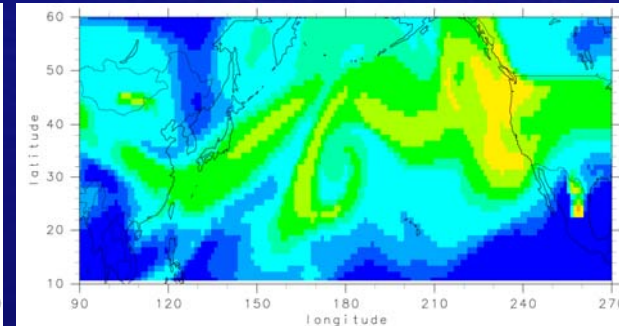
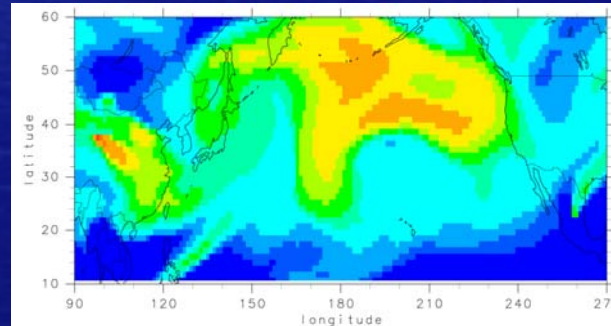
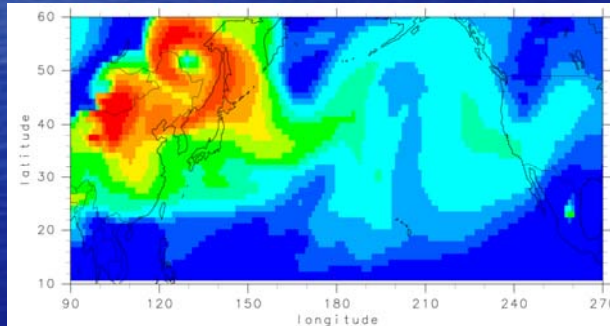
April 12

April 14

TOMS aerosol index (NASA GSFC)



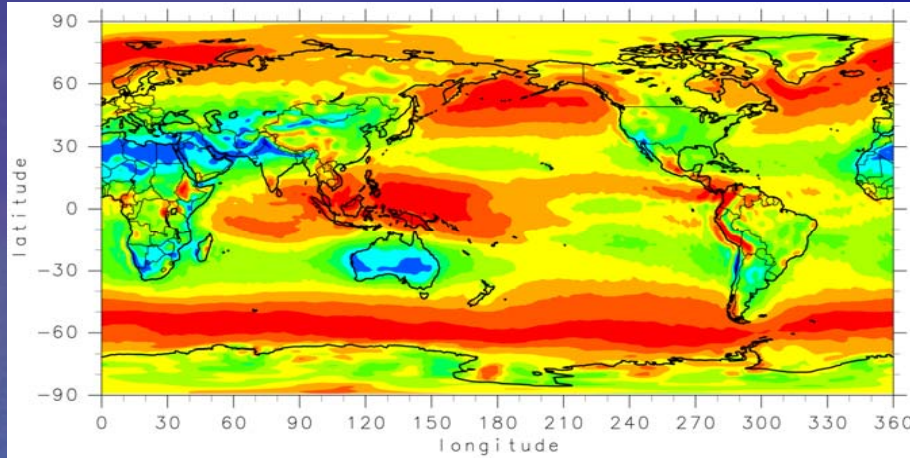
SPRINTARS optical thickness (dust)



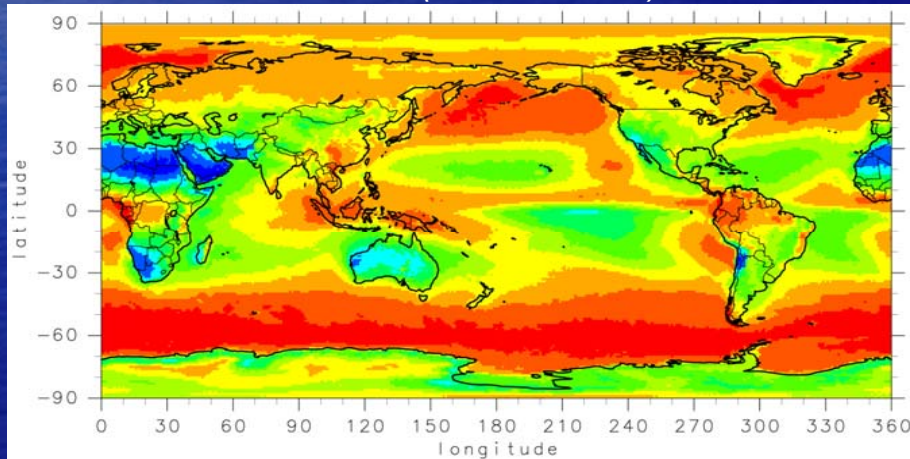
TOMS aerosol index (top) and SPRINTARS optical thickness of soil dust (bottom) on April 8, 12, and 14, 2001 over the northern Pacific region (*Takemura et al. 2002*).



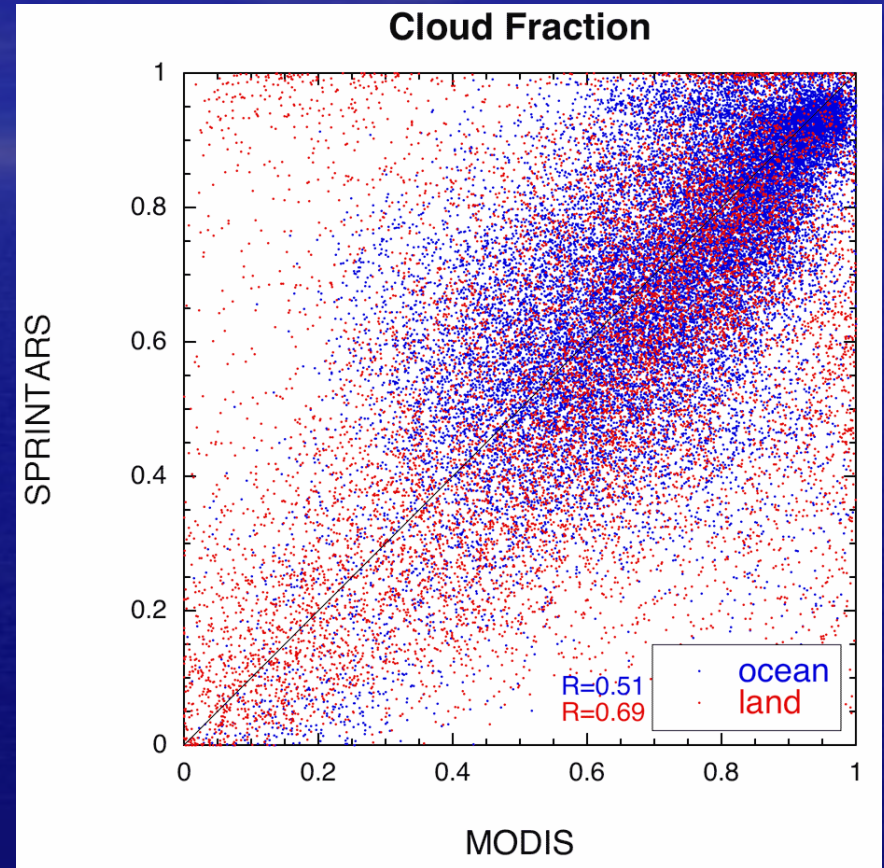
# Comparison of cloud fraction SPRINTARS



**MODIS** (NASA GSFC)



Annual mean distributions of the cloud fraction by SPRINTARS (top) and MODIS (bottom).



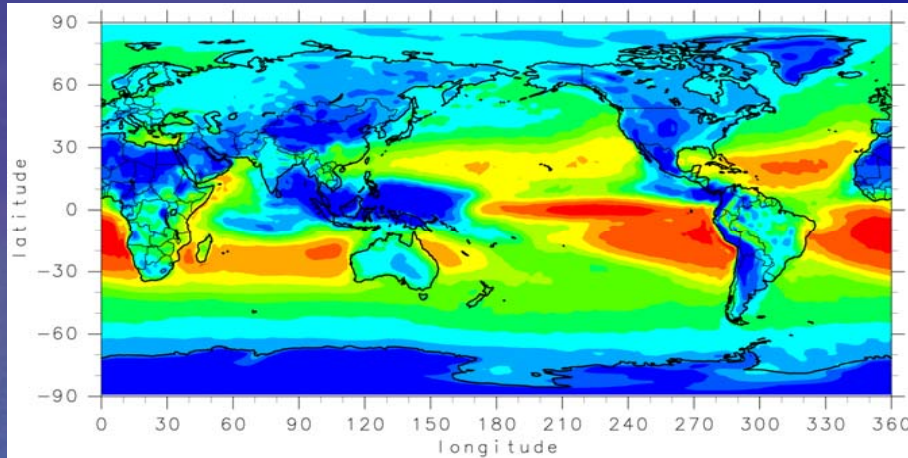
$10^\circ \times 10^\circ$ , 2000-2004

Comparison of monthly mean cloud fraction between MODIS and SPRINTARS.

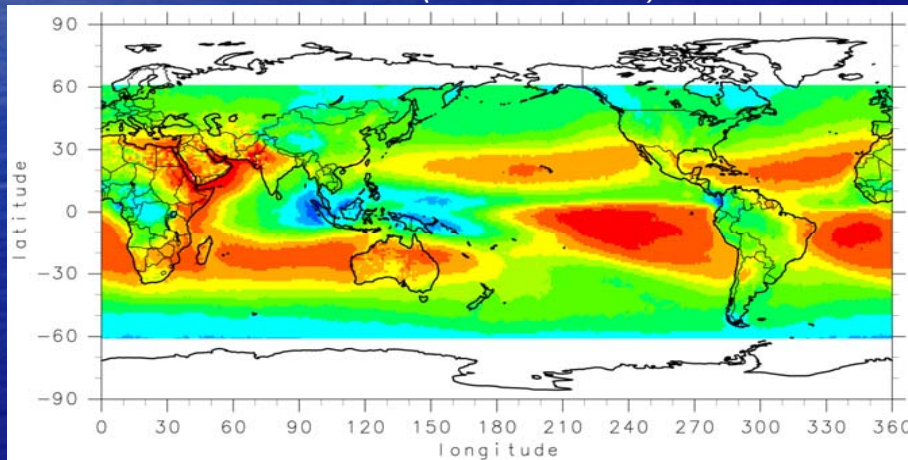


# Comparison of cloud top temperature

SPRINTARS



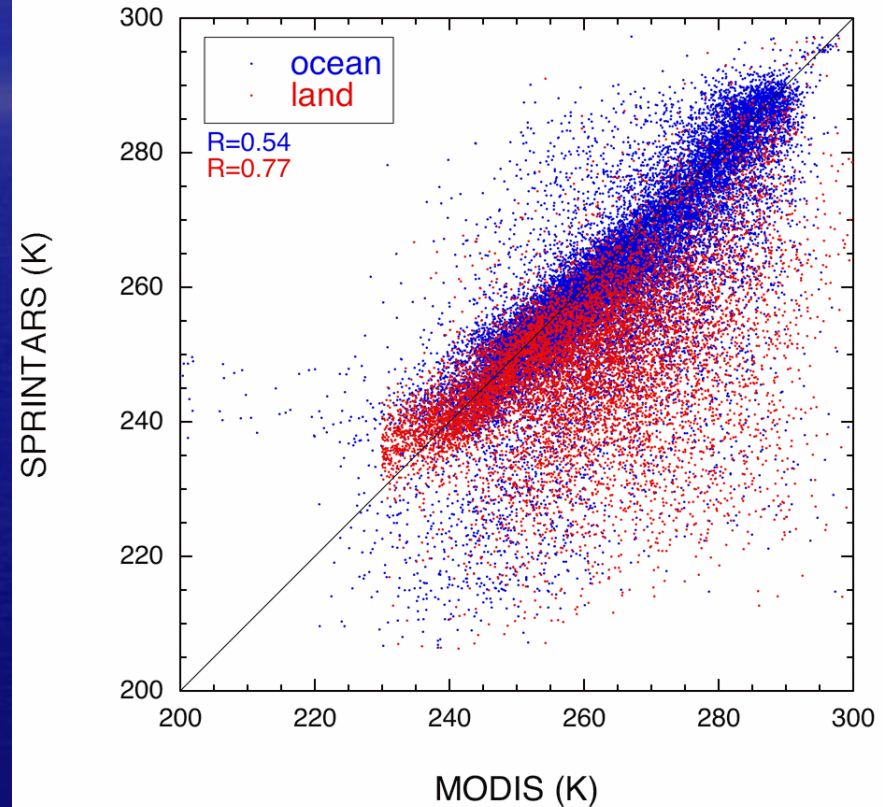
MODIS (NASA GSFC)



240 250 260 270 280 290 (K)

Annual mean distributions of the cloud top temperature by SPRINTARS (top) and MODIS (bottom).

## Cloud Top Temperature

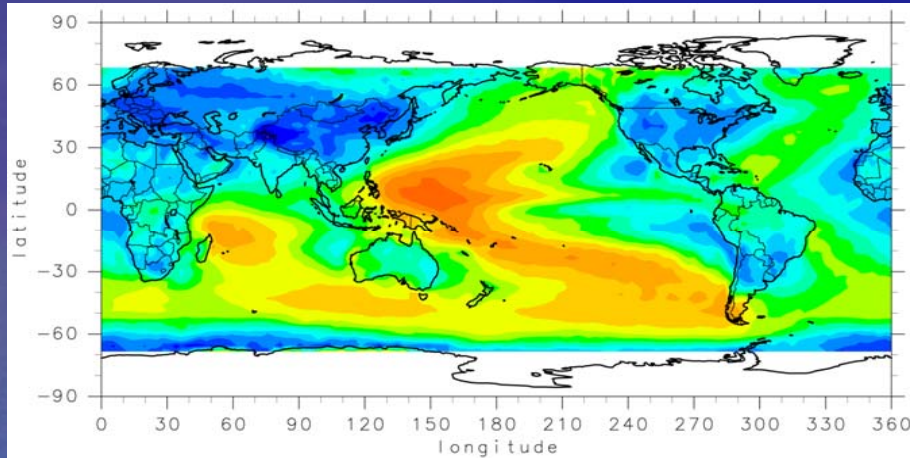


$10^{\circ} \times 10^{\circ}$ , 2000-2004

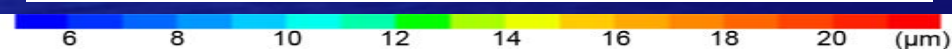
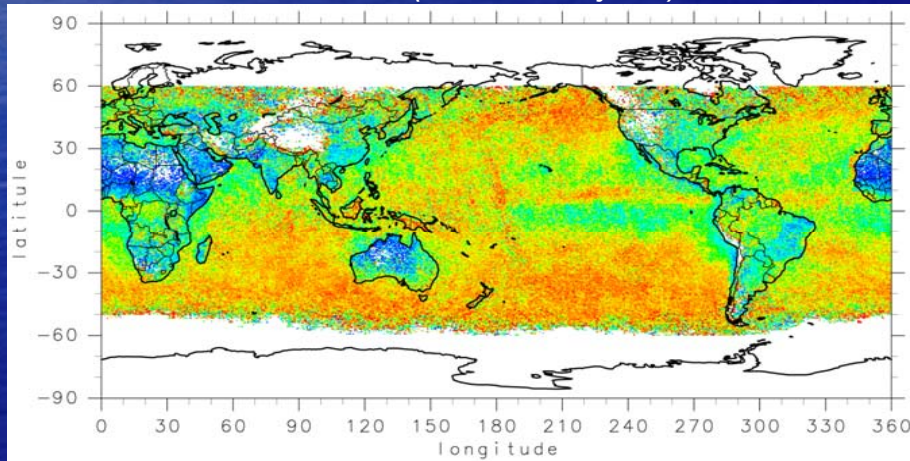
Comparison of monthly mean cloud top temperature between MODIS and SPRINTARS.



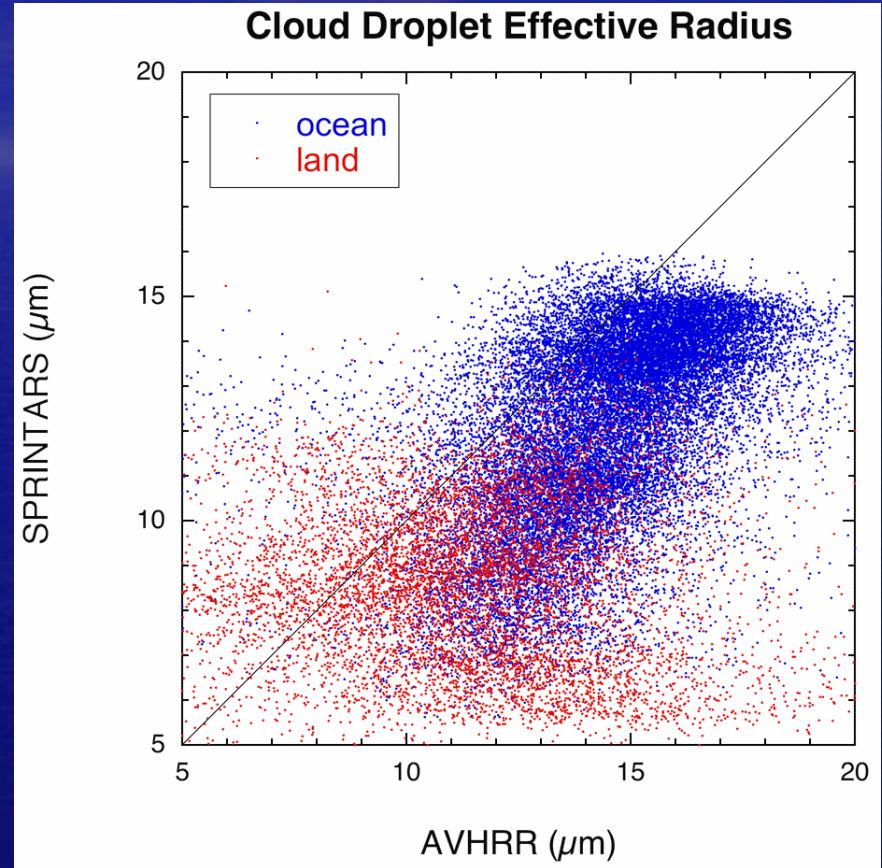
# Comparison of cloud droplet effective radius



AVHRR (T. Y. Nakajima)



Annual mean distributions of the cloud droplet effective radius at cloud top by SPRINTARS (top) and AVHRR (bottom).



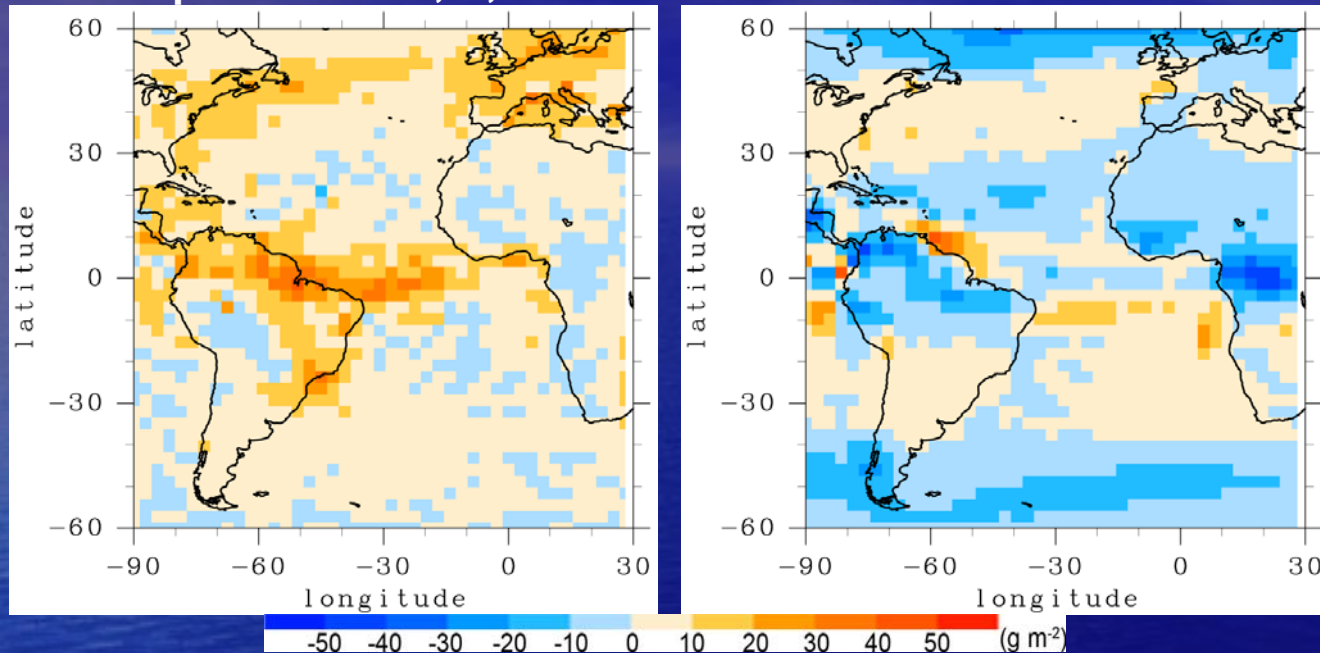
1.1° x 1.1°  
1990 (AVHRR), 2000-2004 (SPRINTARS)

Comparison of monthly mean cloud droplet effective radius at cloud top between AVHRR and SPRINTARS.



# Aerosol effects on clouds

Change in cloud water path by anthropogenic aerosols  
prescribed U, V, T      with slab ocean



Change in the simulated cloud water path due to aerosols from preindustrial to present days with prescribed wind and temperature (left) and with a mixed-layer ocean model (right).

(左) 人為起源エアロゾル増加に対する雲微物理過程の応答

→ 雲水量増加 (エアロゾル第2種間接効果)

(右) 人為起源エアロゾル増加による直接・間接効果に伴う

- ・ 地表付近での太陽放射量減少 → 地表面からの水蒸気蒸発量減 → 雲水量減少
- ・ 水循環の変化

## Next

### step

§ モデルによる雲・エアロゾルの鉛直分布を能動センサによる観測と比較

- ・ 地上や船舶からのレーダー・ライダー観測
- ・ 人工衛星からのレーダー・ライダー観測

ex.

§ 全球モデルでのエアロゾルを明に含めた氷雲過程の表現

- ・ 人為起源エアロゾルによる雲氷量・雲氷サイズ・降水量の変化等

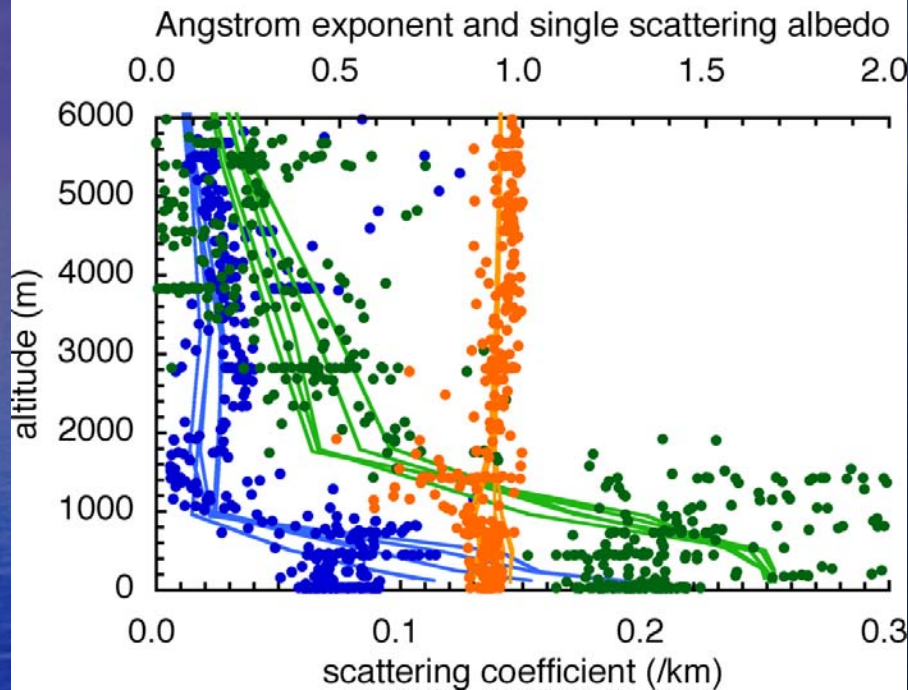
§ 雲をより詳細に表現可能なモデル（非静力学モデル, binモデル等）とエアロゾルモデルとの融合

- ・ NICAM (FRCGC/CCSR) + SPRINTARS
- ・ [NHM + HUCM] (CCSR) + SPRINTARS
- ・ エアロゾルモデルから出力されたエアロゾル分布（エアロゾル種別の数濃度・粒径分布）を雲・降水過程に着目している研究者へ提供



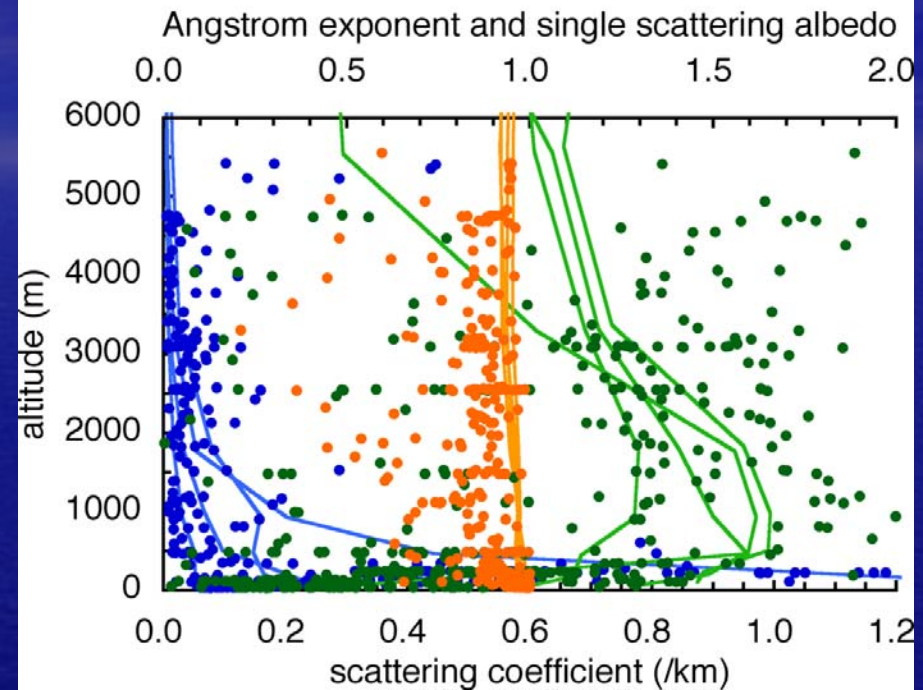
# Aerosol vertical profile

C130 Flight 12 (23 April 2001)



West Japan

C130 Flight 16 (30 April 2001)



Southwest Japan

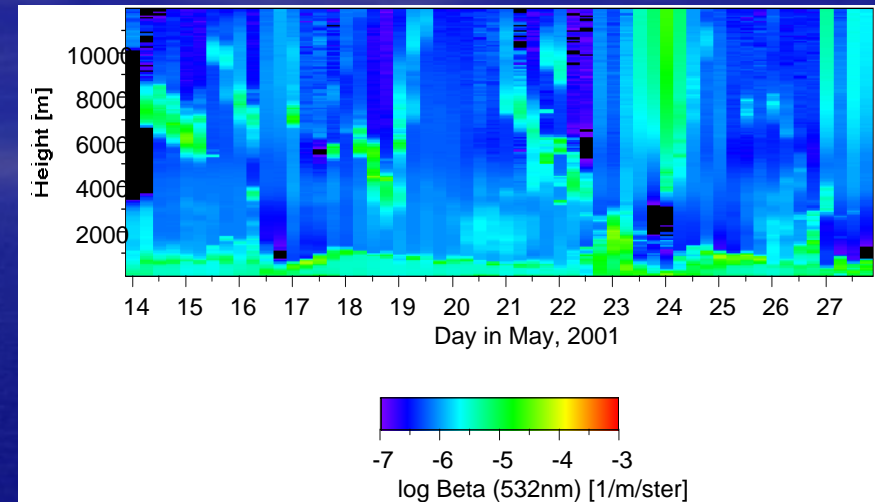
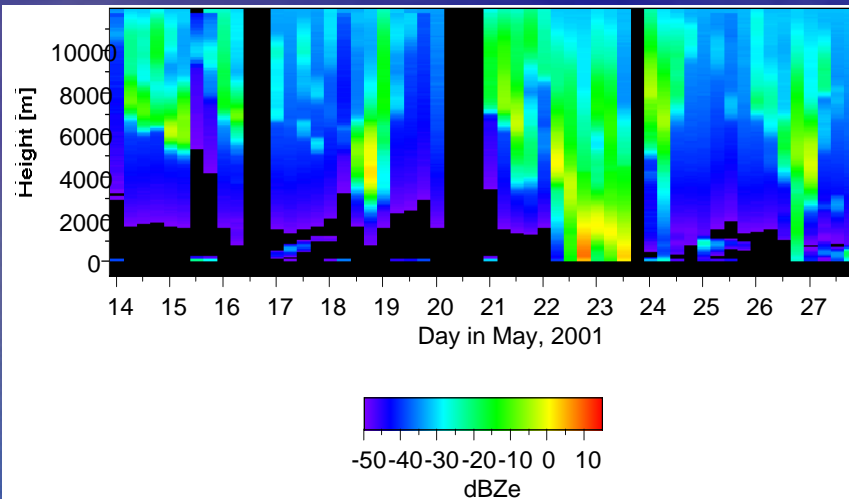
Vertical profiles of the aerosol scattering coefficient (blue), Ångström exponent (green), and single scattering albedo (red) simulated by SPRINTARS (lines) and observed by C-130 (dots) during ACE-Asia. (C-130 data by courtesy of Prof. T. Anderson) (Takemura *et al.* 2003).

# Vertical profiles of aerosols and clouds

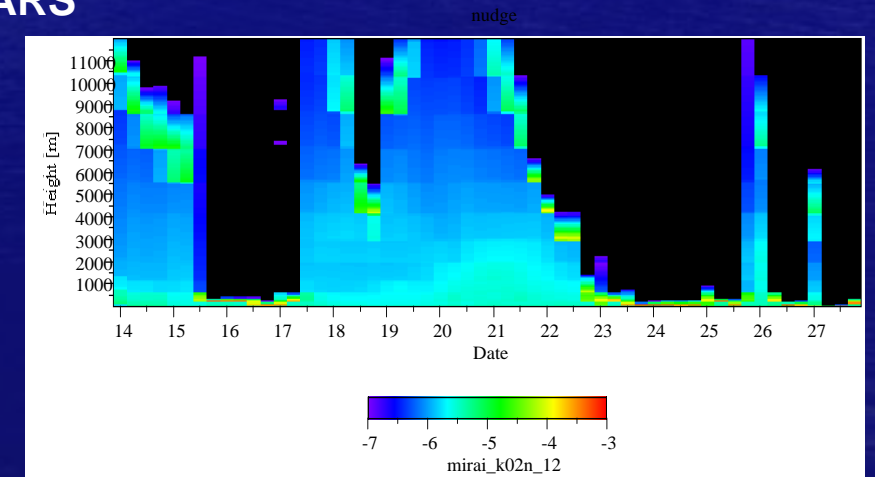
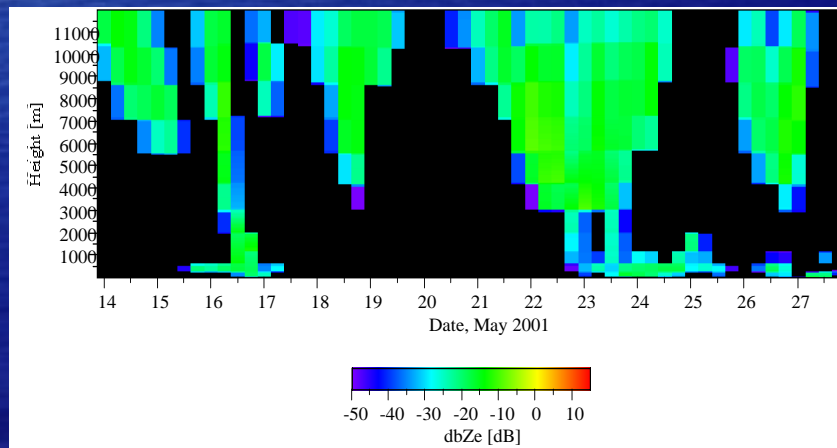
Radar

Lidar

Observation (MR01-K02)



SPRINTARTS



Vertical profiles of radar and lidar signals observed during MIRAI MR01-K02 cruise (top) (*Okamoto et al.*) and simulated by SPRINTARTS (bottom).